

Curing characteristics and internal stresses in epoxy coatings: Effect of crosslinking agent

A. F. ABDELKADER

Technical Department, Fosroc Saudi Arabia, PO Box 11081, Jeddah, 21453, KSA

J. R. WHITE*

School of Chemical Engineering and Advanced Materials, Herschel Building, University of Newcastle upon Tyne, Newcastle upon Tyne, NE1 7RU, UK

E-mail: jim.white@ncl.ac.uk

The development of internal stresses in a series of epoxy coatings prepared using five different crosslinking agents have been studied. The crosslinking agents were: H1, 4,4' methylenedianiline (DDM); H2, diethylentriamine (DETA); H3, cycloaliphatic polyamine; H4, polyaminoimidazoline; and H5, polyamidoamine adduct. Four different post-cure treatments were applied and the dependence of internal stress on crosslinking agent and post-cure treatment was determined. Curing was followed by monitoring the FTIR epoxy band at 916 cm^{-1} and the glass transition temperature was determined using DSC to assist interpretation of the measured values of internal stress. The internal stress was tensile in all of the materials at the end of each post-cure treatment. The stress magnitudes increased monotonically with post-cure temperature. The largest stresses were recorded with H1, H2 and H3 whereas the lowest stresses were recorded with H4 and H5, which both included a flexible aliphatic chain. The effects of ageing for extended periods in dry air and in humid air (52%RH and 97%RH) were also examined. Exposure to humid air almost always caused a reduction in the tensile stress and often produced compressive stresses, attributed to swelling due to water absorption. A comparison was made of the stresses formed in coatings applied to a thin substrate that was (i) free to bend during curing, post-curing and ageing, and (ii) prevented from bending ("restrained substrate"). The general trends in behaviour were in agreement but no simple relationship could be found between the stress magnitudes obtained by the two different test configurations.

© 2005 Springer Science + Business Media, Inc.

1. Introduction

The development of internal stresses¹ in organic coatings is recognised as a major contributor to failures [2–6]. The stresses present immediately after the solidification of a coating on a substrate are normally tensile. High levels of internal stress can affect coating adhesion and may provoke delamination or cracking [2]. Studies of internal stresses in a wide range of polymeric coatings have been reviewed elsewhere [7]; studies of internal stresses in epoxy coatings have included investigation of solvent-borne epoxies [8, 9] and solvent-free systems [10, 11]. Factors affecting the magnitude of internal stresses in coatings include the film-formation process [12–19], exposure to moisture and changes in temperature [8, 20–22] and cycles of water immersion and drying out [20, 23]. Post-curing conditioning can

cause the internal stress in the coating to reverse, becoming compressive.

The curing characteristics of epoxy resins have been studied extensively but there are few studies of the effect of curing agent and curing conditions on the development of internal stresses. The source of the stresses may be one of several processes or a combination of more than one. One source is contraction associated with molecular rearrangements during crosslinking or physical ageing, and this is likely to be affected by the molecular structure and bonding mechanism of the curing agent. Stress relaxation during curing and after its completion has a strong influence on the level of internal stress that is observed. The rate and amount of relaxation depend on the glass transition temperature, T_g , and this is dependent on the nature of the epoxy

*Author to whom all correspondence should be addressed.

¹ The term "internal stress" is used to describe the self-stressed state in a coating-substrate system that develops when the coating expands or contracts against the restraining influence of the stiffer substrate. It therefore resembles "residual stresses" in fabricated polymers such as injection mouldings, for which the term "internal stress" may represent other phenomena [1]. The terms "internal stress" and "residual stress" are often used interchangeably in the coatings community.

curing agent, the extent of cure, and on the conditions (temperature; the presence of a penetrant such as water that may act as a plastifier). The rate of change of internal stress therefore changes throughout the curing process and relaxation does not necessarily terminate when curing is complete. If the epoxy resin is applied to a substrate as a coating, and if an elevated temperature is used during curing, the internal stress also depends on the differential thermal contraction between coating and substrate. Finally, the mechanical constraints that are present when the curing process occurs have a strong influence on the magnitude of the stress that develops [19].

It is important to know the magnitude and causes of internal stresses in coatings because they may be sufficient to promote cracking or delamination from the substrate. The results reported here are taken from a comprehensive study of a family of epoxy coatings based on the same resin and using five different curing agents [7]. The coatings were cured at four different temperatures then aged at room temperature, using three different humidity levels. The coatings were applied to thin substrates that bent considerably during curing if allowed to ("free-to-bend") and this resulted in different stress level than those which developed if the substrates were held flat during curing ("restrained substrate method") [19]. Samples were cured in both "free-to-bend" and "restrained substrate" configurations for comparison.

2. Experimental

2.1. Materials

The epoxy resin and the hardeners used in the experiments reported here along with the mix ratios are shown in Table I. The materials used in this investigation were based on the epoxy resin DER 331[®] (DOW Chemical Co.), an undiluted diglycidyl ether of bisphenol A (DGEBA)-based liquid with an epoxy equivalent mass of 182–192 g/mol. It is fairly typical of low molecular mass epoxy resins that have become standard because of their versatility in many coating applications.

Five different types of amine curing agents were used in this study in conjunction with the epoxy resin (EP). The curing agents were: 4,4'-diaminodiphenylmethane (DDM) (H1); diethylenetriamine (DETA) (H2); cycloaliphatic amine based on isophorone diamine (IPD) (H3); polyaminoimidazoline based hardener (H4); and polyamidoamine based adduct hardener (H5). The chemical structures of the hardeners together with the

mix ratios for the compositions used in this study are given in Table I.

2.2. Mixing procedure

Curing agents H2–H5 are liquid at room temperature and the mixtures with the epoxy resin were made in batches of 100 g under vacuum using a mechanical paddle stirrer. Each batch was mixed for about 3 min at moderate speed, then allowed to stand for 5 min before application to the substrate.

Curing agent H1 is a solid at room temperature, and a different mixing technique was required to obtain a mixture suitable for use as a coating at ambient temperature. The procedure adopted was to melt the required amount of H1 at 100°C and mix it with an equal mass of EP at this temperature. Then the mixture was added to the remainder of the EP resin at room temperature and mixed under vacuum to get the final mix at a temperature of about 35°C. Even though the material started slightly above ambient temperature at the commencement of application, the coated substrate reached room temperature ($23 \pm 1^\circ\text{C}$) within a period of <2 min (confirmed using an IR thermometer). That means that vitrification took place at room temperature as in the case of the mixtures based on the liquid curing agents.

2.3. Sample preparation

The research concerns the properties of the epoxy materials when used as coatings and the mixtures prepared as described in Section 2.2 were applied to steel shim substrates 0.1 mm thick and with the coated area measuring 150.0 mm × 23.0 mm. The reason for using thin substrates was to facilitate measurement of the internal stress in the coating by the bending beam procedure [7, 19]. Prior to coating, the shims were de-greased using MEK (methyl ethyl ketone). During the coating operation, the shims were held flat on a horizontal glass sheet. The coating was applied using a 6 mm paint brush. A strip 5 mm at each end of the shims was left uncoated. The research programme from which the results described here are extracted included a detailed comparison of the development of internal stresses when the substrate was held flat and when it was free to bend during curing and subsequent ageing [19]. The stress magnitudes that are measured when the substrate is free to bend are significantly higher than those measured when

TABLE I Material compositions

Code	Material	Grade	Commercial name	Supplier	Mix ratio (phr) ^a
EP	Diglycidyl ether bisphenol A	Commercial	DER 331	Dow Chemical	
H1	4,4' methylenedianiline (DDM)	Lab	–	Acros Organics	26 ^b
H2	Diethylenetriamine (DETA)	Commercial	–	UC/Dow Chemical	11 ^b
H3	Cycloaliphatic polyamine	Commercial	Aradur 42	Huntsman	22 ^c
H4	Polyaminoimidazoline	Commercial	Aradur 140 BD	Huntsman	50 ^c
H5	Polyamidoamine adduct	Commercial	Aradur 450 BD	Huntsman	60 ^c

^aParts per hundred parts of epoxy resin (EP) by weight.

^bStoichiometric ratio.

^cAs recommended by the manufacturer.

the substrate is restrained and results obtained using both procedures will be given below (clearly identified). Immediately after preparation the free-to-bend samples were placed onto a pair of 4 mm diameter round bars with separation chosen so that the bending moments due to the gravitational forces balanced each other to minimise bending of the assembly under its own weight (the “double-overhang method”) [7, 19, 24, 25]. Restrained samples were prepared on identical substrates but were fastened tightly onto a flat rigid surface during curing and released periodically for short periods to make a curvature measurement [7, 19].

The coatings used throughout this study were neat epoxy systems, free from fillers or rheology modifiers, and the coatings were self-smoothing, forming a uniform thickness across the substrate. The thickness of the coatings ranged between 0.7 and 0.9 mm. Immediately after the coating application, the samples that were to be cured and aged in the restrained state were clamped onto steel blocks 150.0 mm × 23.0 mm × 10 mm at each end using G-clamps [7, 19]. All samples were then left to have an initial cure at room temperature for 24 h in an enclosure containing silica gel to ensure that moisture did not affect this part of the curing process.

Samples for thermal analysis by differential scanning calorimetry (DSC) were made in the same way but coated onto a Teflon® substrate (100 mm × 100 mm). The coatings (0.7–0.9 mm thick) were removed from the substrate for the post-curing operation (see below). Small pieces (3–4 mm diameter) were used for the DSC measurements.

2.4. Curing, post-curing and storage conditions

After the initial cure (24 h at 23 ± 1°C and 0%RH) the samples were divided into four groups and each group then was subjected to a different post-cure treatment as follows:

C1: continued curing at 23°C in a dry atmosphere for 4 weeks;

C2: 24 h at 55°C;

C3: 12 h at 75°C;

C4: 4 h at 150°C.

The post-curing treatments at elevated temperature were conducted in an air-circulating oven accurate to ±1°C. At the end of the post-curing period, cooling was conducted in the oven; the rate of cooling in the region of the glass transition temperature was $-2.0 \pm 0.5^\circ\text{C}/\text{min}$. At the end of the cooling phase, the samples were divided into three sub-groups and transferred to chambers maintained at relative humidity levels 0, 52 and 97% respectively.

2.5. FTIR and DSC measurements

Fourier transform infrared (FTIR) measurements on newly mixed samples were made using samples prepared by squeezing a drop of the mixture between two 1 mm thick KBr discs. Measurements on cured ma-

terial were made on samples removed using a sharp knife, ground with KBr and pressed into a disc. The FTIR spectra were recorded using a Nicolet 20PC-IR instrument in the wavenumber range 500–4000 cm^{-1} . The epoxy group band at 916 cm^{-1} was used to follow the progress of curing.

The DSC measurements were made using a Mettler TA89A Differential Scanning Calorimeter. Pre-weighed samples cut from the free films (see Section 2.3) were tested in 40 μl aluminium crucibles sealed with a lid. A heating rate of 10°C/min was used for scans from 25 to 150°C (sometimes to 180°C). The glass transition temperature, T_g , was taken to be the extrapolated onset temperature, following ASTM method D3418-75 [19, 26]. The preliminary thermal cycle recommended in the test method [26] was omitted because it advances the cure and erases much of the difference in the materials prepared using the different post-cure treatments. Triplicate DSC scans were run and the T_g values reported below are each the average of three results, with repeatability $\pm 1.5^\circ\text{C}$.

2.6. Internal stress measurements

2.6.1. Curvature measurement

The internal stress in the coating was derived from the curvature of the substrate-coating combination when it was freed from external tractions and allowed to reach moment equilibrium. Samples that were restrained during curing were released from the steel block only during the curvature measurement process. This is essential as any prolonged duration in the unrestrained state would enable curing and stress relaxation to take place under different conditions. In the experiments described here, the measurement was carried out within 5 min of releasing the sample. In a separate series of experiments, the unrestrained dwell time was extended to 15 min to attempt to determine the sensitivity of the measurement to this factor. No measurable change in curvature developed in the extended period. To measure curvature, the samples were clamped lightly in one location so that they were free to bend with the width direction vertical, and held above a piece of white paper. The contour of the curved surface was copied onto the paper and the curvature determined using standard geometric measurements. With this arrangement, there was no gravitational contribution to bending. Three samples were used for each combination of composition and condition. The reproducibility of the curvature measurements was good and when converted to stress, as reported below, the standard deviation was ≤ 0.1 MPa.

2.6.2. Internal stress evaluation

For a coating with Young’s modulus E_c , Poisson ratio ν_c and thickness a on a substrate with Young’s modulus E_s , Poisson ratio ν_s and thickness b , the relationship between the radius of curvature R and the internal stress in the coating σ_c is given by [9]:

$$\sigma_c = \{a E_c / 6R(1 - \nu_c)\} \{ (1 + 4\alpha\beta + 6\alpha^2\beta + 4\alpha^3\beta + \alpha^4\beta^2) / (1 + \alpha)(1 + \alpha\beta) \} \quad (1)$$

where $\alpha = b/a$ and $\beta = \{E_s/E_c\}\{(1 - \nu_c)/(1 - \nu_s)\}$. This form of the relationship between the residual stress and the curvature takes account of the true position of the neutral surface of the substrate-coating combination, which is displaced slightly from the mid-plane of the substrate. In a majority of the analyses presented in the literature, the treatment is simplified by taking the neutral surface to be exactly at the mid-plane of the substrate. The approximation incurred by this practice becomes progressively worse as the ratio of coating thickness to substrate thickness increases.

For the calculations presented here, E_c and E_s were taken to be 3400 MPa and 200 GPa respectively and ν_c and ν_s were taken to be 0.34 and 0.29 respectively.

3. Results

3.1. FTIR

The progress of curing at 23°C was monitored using FTIR. Fig. 1 shows the results for (a) EP/H1 and (b) EP/H4. The epoxy band at 916 cm⁻¹ diminished progressively with time and in EP/H1 was very weak after 200 days. A similar result was obtained with EP/H2 and EP/H5 [7]. With EP/H3 and EP/H4 the 916 cm⁻¹ band was still significant after 200 days [3], though very small (Fig. 1b). Curing using conditions C4 caused the epoxy band to disappear altogether for all mixes, indicating that curing was complete (Fig. 2).

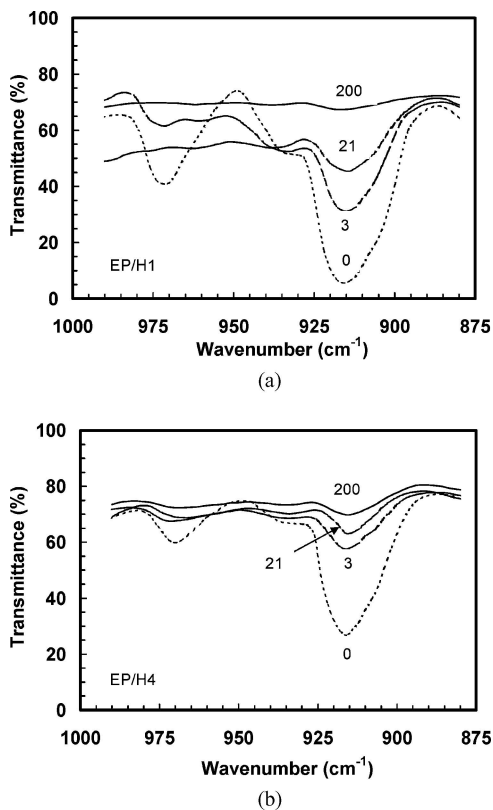


Figure 1 FTIR spectra for (a) EP/H1 and (b) EP/H4 cured in dry air at 23°C for various periods of time, given in days on the corresponding lines.

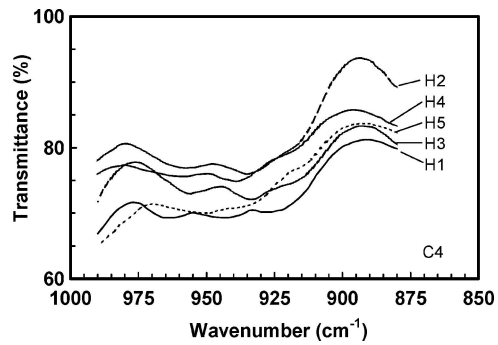


Figure 2 FTIR spectra for all five compositions following post-cure treatment C4.

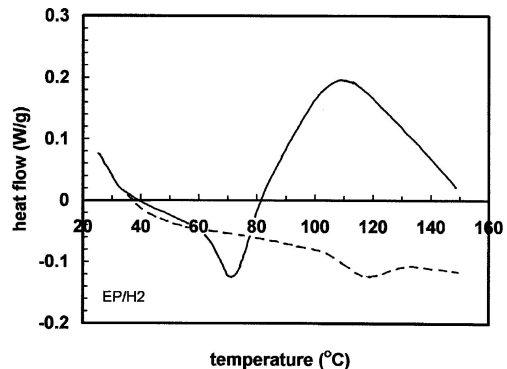


Figure 3 DSC runs for EP/H2. Solid line: first run; broken line: second run.

3.2. DSC

3.2.1. General characteristics

Fig. 3 shows the results of a first heating run on a sample of composition EP/H2 cured under conditions C1 (room temperature cure in a dry atmosphere) plus a second heating run on the same sample, conducted after cooling it in the DSC equipment. In the first heating run there is an endothermic transition just above 70°C, attributed to the glass transition, followed by an exotherm, attributed to continued curing. The exotherm was particularly prominent with samples allowed to cure at room temperature, indicating that they were significantly under-cured at the commencement of the first DSC run. Heat treatment in the DSC advances curing very considerably and the second heating scan produced a very different characteristic (Fig. 3) showing that the T_g had increased to ~120°C and the post- T_g exotherm had disappeared. This confirms that information about the original state of the material immediately after the post-curing phase is lost by the time the second heating run is conducted (Section 2.5).

3.2.2. Effect of post-cure treatment

An example of the effect of the post-cure treatment on the DSC signature is given in Fig. 4 for composition EP/H3. The glass transition temperature, T_g , is taken to be at the minimum in the thermogram. It is evident that the higher the post-cure temperature, the higher is T_g . The T_g measurements made in this way for all five compositions and for all four post-cure treatments are given in Fig. 5. Samples made with hardener H1 have the highest values of T_g for all post-cure treatments and

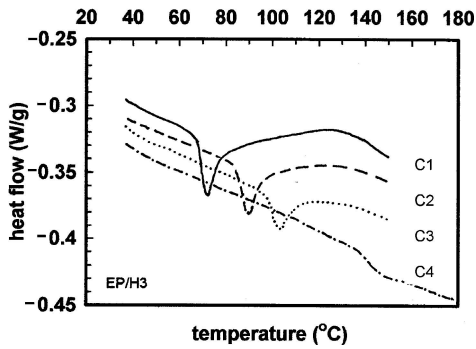


Figure 4 DSC results for EP/H3 after different post-cure treatments.

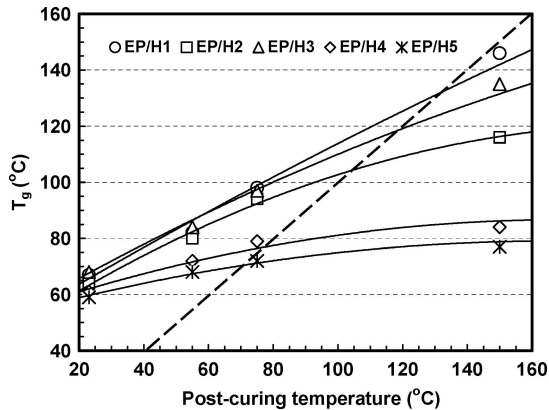
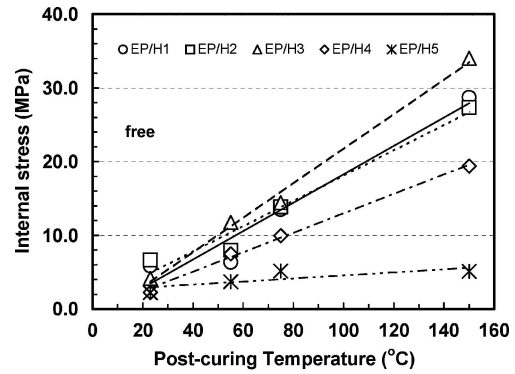


Figure 5 T_g values obtained from DSC runs on all five materials and for all four post-cure treatments, plotted versus the post-cure temperature, T_c . The broken line shows the condition $T_g = T_c$.

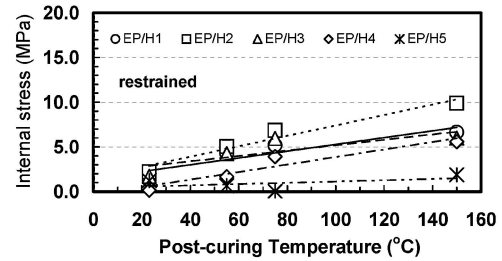
those made with hardener H5 have the smallest values of T_g . The samples containing H4 behaved fairly similarly to those containing H5 whereas those containing H3 were fairly similar to those containing H1. Fig. 5 shows that for room temperature post-cure the T_g s for the five hardeners cover a rather narrow range (~ 59 – 68°C) whereas for post-curing at 150°C (C4) the T_g range spans from 77 – 146°C , showing high sensitivity to the curing agent used.

3.3. Internal stress immediately after the post-cure treatment

Fig. 6 shows the stress levels measured at the completion of the post-cure treatment, as soon as the substrate-coating combination had returned to room temperature equilibrium. Results are given for (a) free-to-bend samples and (b) restrained substrate samples. The stresses recorded for the free-to-bend method are very much higher than those obtained with the restrained substrate procedure. The stress levels increased monotonically, quasi-linearly, with post-cure temperature. The stress magnitudes were strongly dependent on the hardener used. The lowest values of stress were recorded for EP/H5 by both methods, reaching ~ 3 MPa in the free-to-bend sample for condition C4 and ~ 1 MPa for the restrained substrate sample. EP/H3 had the highest stresses recorded for free-to-bend samples whereas EP/H2 gave the highest values with restrained substrate tests. This confirms that there is no simple universal re-



(a)



(b)

Figure 6 Equilibrium internal stress values measured just after completion of the post-cure treatment (a) free-to-bend measurements; (b) restrained substrate measurements.

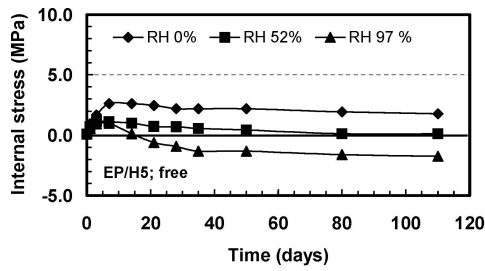
lationship between free-to-bend curing and restrained substrate curing, reflecting the complex events that occur during curing [19].

3.4. Effect of room temperature ageing at different RHs on internal stress

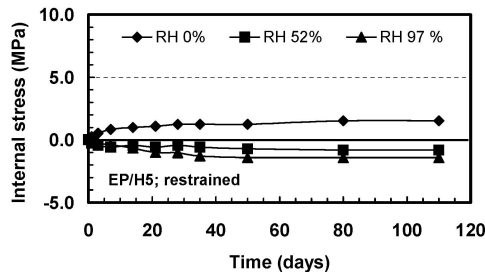
3.4.1. Post-cure condition C1 (4 weeks at 23°C , dry atmosphere)

A series of measurements were made on samples that were cured for 24 h in a dry environment, cured for a further 4 weeks in a dry atmosphere at 23°C , then stored at 23°C at different relative humidity levels for an extended period of time. Fig. 7 shows the development of internal stress in EP/H5 over a period of almost 3 months. The stresses obtained with the free-to-bend technique were again higher than those on the restrained substrate. Similar data have been presented previously [19] for EP/H1 and EP/H2, though the stress values reported were in error (they were too small, by a factor of 10). For restrained substrate samples, the stress at the commencement of the storage period was very small, and tensile if measurable, for all five materials, consistent with the results presented in Fig. 6. Some of the free-to-bend samples possessed quite significant stresses at the commencement of the storage period, again consistent with the results shown in Fig. 6. The tensile stress in all of the samples stored at 0%RH proceeded to increase with storage time, levelling out after about 50 days.

The EP/H5 coating conditioned at room temperature at 97%RH quickly developed compressive stresses whether tested in the free-to-bend or restrained substrate condition (Fig. 7). The same was observed with coatings made using all five hardeners [7]. When EP/H5

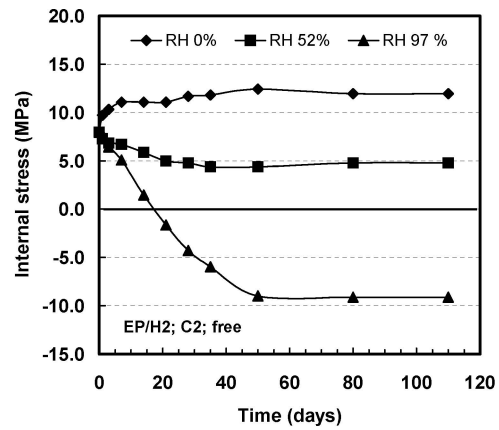


(a)

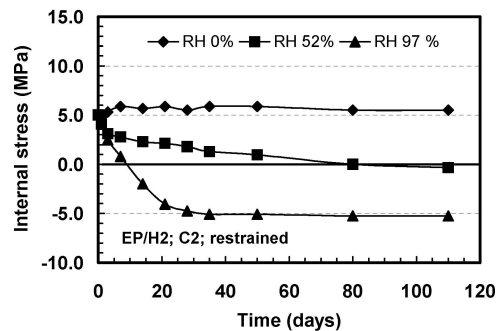


(b)

Figure 7 Internal stress development in EP/H5 cured in a dry environment for 23°C then stored at 0; 52; 97%RH. (a) Free-to-bend measurement; (b) restrained substrate measurement.



(a)



(b)

Figure 9 Internal stress development in EP/H2 post-cured using conditions C2 then stored at RH 0; 52; and 97% respectively. (a) Results obtained with free-to-bend substrate; (b) results obtained with restrained substrate.

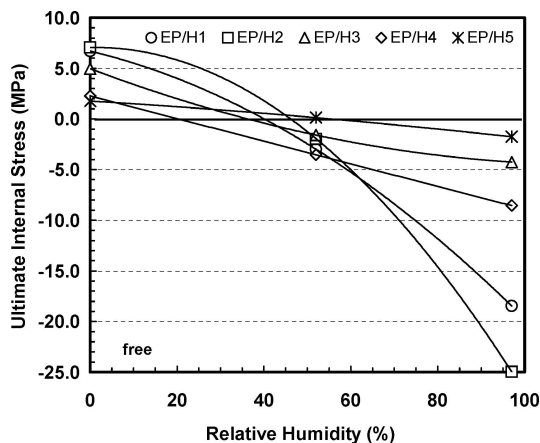


Figure 8 Effect of relative humidity on the equilibrium (long ageing time) stress built up in coatings on free-to-bend substrates stored at 0; 52; and 97%RH after post-curing for 24 h in a dry atmosphere at 23°C. The equivalent data for restrained substrate testing are given in references 7 and 19.

was aged at 52%, the stress on the free-to-bend substrate levelled out at a value that was impossible to separate from zero (Fig. 7). The other coatings (EP/H1-4) all developed compressive stresses when conditioned on a free-to-bend substrate (Fig. 8). When conditioned at 52%RH on a restrained substrate all five coatings developed compressive stresses [7, 27]. The development of compressive stress is probably caused by water absorption, leading to swelling of the coating. The water is likely to plasticize the coating, facilitating relaxation. It is evident that swelling is the dominant effect but it appears that with EP/H5 the effect of relaxation is relatively more influential than with the other coatings.

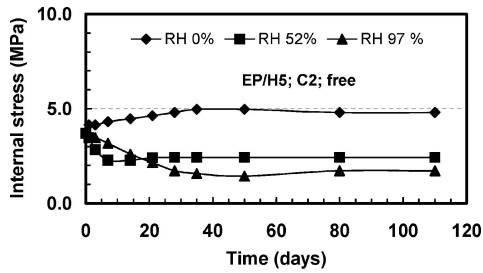
3.4.2. Post cure condition C2 (24 h, 55°C)

Data for samples aged at room temperature at different humidities after post-curing conditions C2 are given

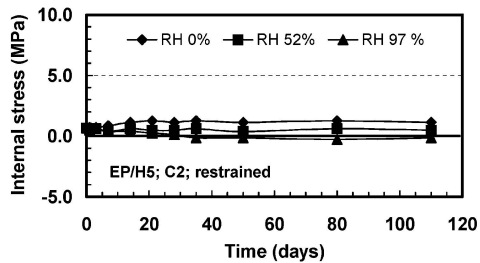
in Figs. 8 and 9. With EP/H2 the stress was already strongly tensile at the end of the post-curing treatment (Fig. 9). Ageing at 0%RH caused the stress to increase still further, to ~12 MPa (free-to-bend substrate) or ~6 MPa (restrained substrate). Ageing at 97%RH caused strong compressive stresses to develop, rising to ~10 MPa (free-to-bend) or ~5 MPa (restrained). The results obtained at 52%RH were intermediate between those for 0% and 97%RH, as expected, with stress levelling out at ~5 MPa tensile (free-to-bend) and ~0 MPa (restrained). The general pattern of the results for EP/H1 and EP/H3 were very similar to those for EP/H2 [7]. The only significant difference was that the equilibrium stress after ageing at 0%RH was lower for EP/H1 (~8 MPa) and higher for EP/H3 (~15 MPa) for free-to-bend testing. The stress changes observed with EP/H5 were much smaller (Fig. 10). The results obtained with EP/H4 were intermediate between those for EP/H1-3 and EP/H5 [7]. The equilibrium stresses obtained for all five configurations for all three ageing conditions are given in Fig. 11.

3.4.3. Post-cure condition C3 (12 h, 75°C)

Fig. 12 shows results obtained on conditioning EP/H2 at the three chosen humidity levels after post-cure treatment C3. The results are fairly similar to those obtained after post-cure treatment C2. Coatings EP/H1 and EP/H3 gave ageing results similar to EP/H2 after post-curing using conditions C3 [7]. When EP/H4 was

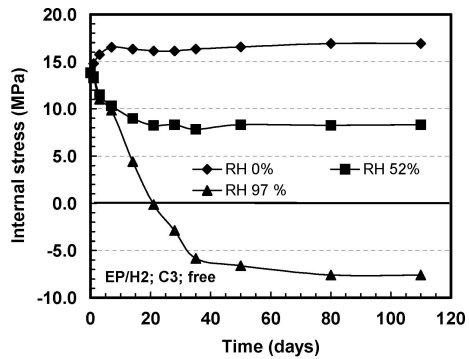


(a)

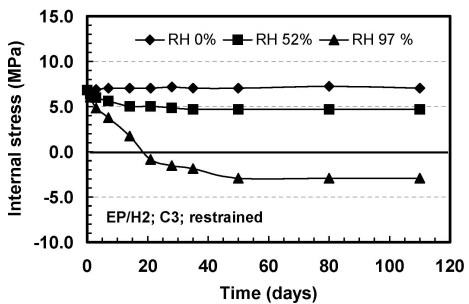


(b)

Figure 10 Internal stress development in EP/H5 post-cured using conditions C2 then stored at RH 0; 52; and 97% respectively. (a) Results obtained with free-to-bend substrate; (b) results obtained with restrained substrate.

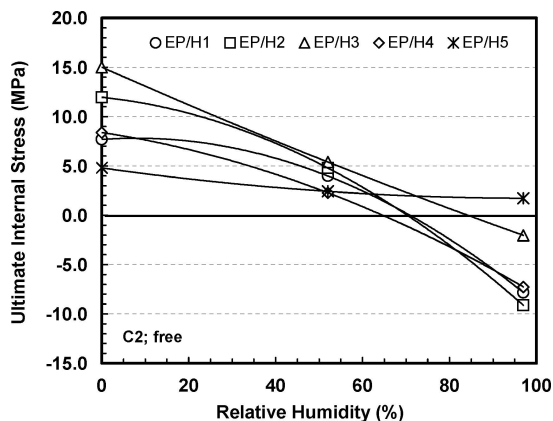


(a)

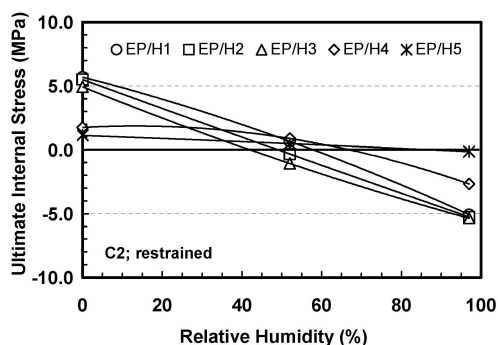


(b)

Figure 12 Internal stress development in EP/H2 post-cured using conditions C3 then stored at RH 0; 52; and 97% respectively. (a) Results obtained with free-to-bend substrate; (b) results obtained with restrained substrate.



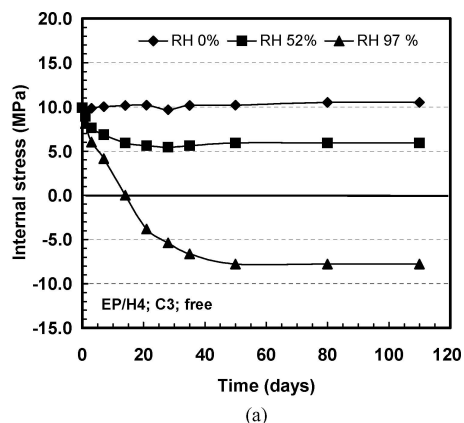
(a)



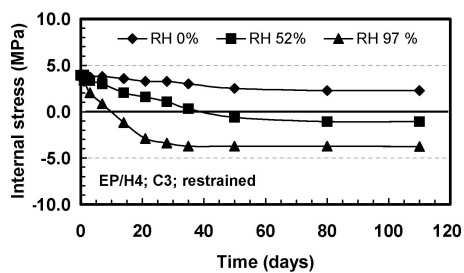
(b)

Figure 11 Effect of relative humidity on the equilibrium (long ageing time) stress built up in coatings on (a) free-to-bend substrates and (b) restrained substrates stored at 0; 52; and 97%RH after post-cure conditions C2.

aged at 52%RH following post-cure C3, a compressive equilibrium stress was obtained (Fig. 13), otherwise its behaviour was similar to that of coatings EP/H1-3. Coating EP/H5 behaved quite differently (Fig. 14). Even at 97%RH the stress in EP/H5 remained tensile on a free-to-bend substrate and on a restrained substrate it actually grew in magnitude (Fig. 14). This result was



(a)

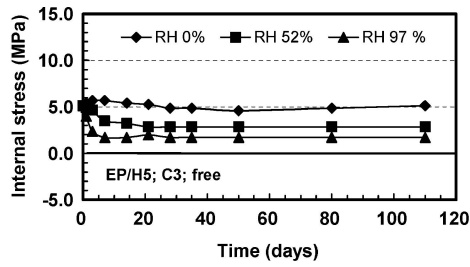


(b)

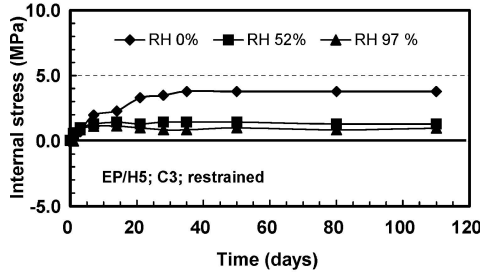
Figure 13 Internal stress development in EP/H4 post-cured using conditions C3 then stored at RH 0; 52; and 97% respectively. (a) Results obtained with free-to-bend substrate; (b) results obtained with restrained substrate.

not observed for any other combination of material and post-cure condition.

The equilibrium stresses obtained using samples after post-cure C3 are summarised in Fig. 15. As with conditions C1 (Fig. 8) and C2 (Fig. 11), EP/H5 showed the least sensitivity to humid atmosphere.

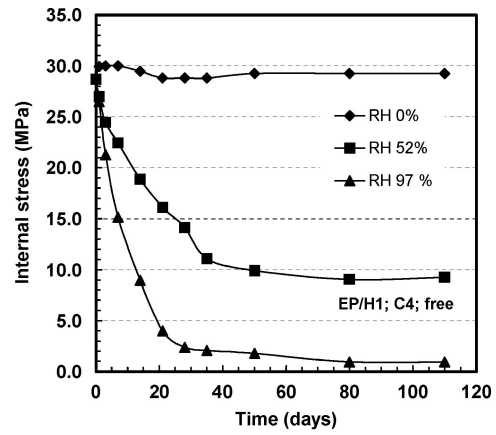


(a)

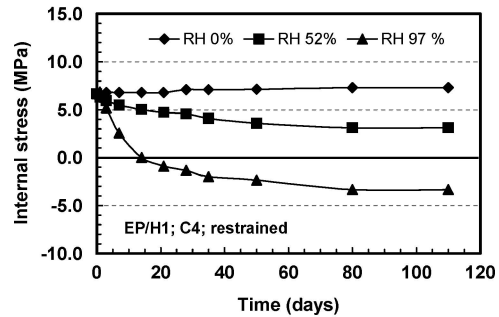


(b)

Figure 14 Internal stress development in EP/H5 post-cured using conditions C3 then stored at RH 0; 52; and 97% respectively. (a) Results obtained with free-to-bend substrate; (b) results obtained with restrained substrate.

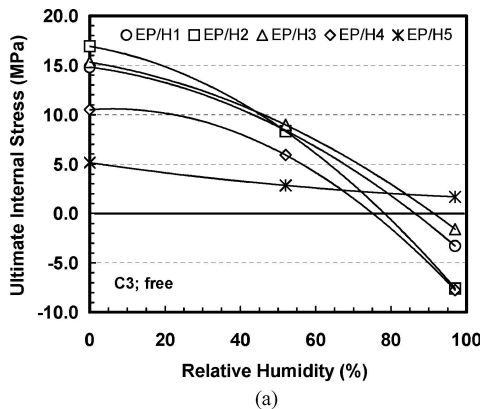


(a)

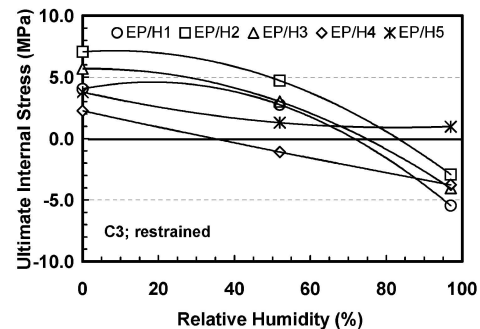


(b)

Figure 16 Internal stress development in EP/H1 post-cured using conditions C4 then stored at RH 0; 52; and 97% respectively. (a) Results obtained with free-to-bend substrate; (b) results obtained with restrained substrate.



(a)



(b)

Figure 15 Effect of relative humidity on the equilibrium (long ageing time) stress built up in coatings on (a) free-to-bend substrates and (b) restrained substrates stored at 0; 52; and 97%RH after post-cure conditions C3.

3.4.4. Post-cure condition C4 (4 h, 150°C)

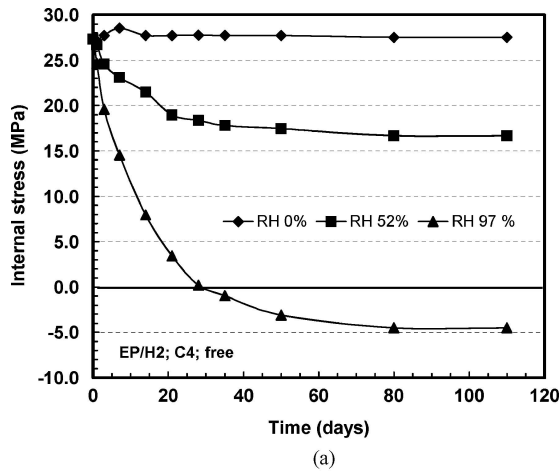
Samples post-cured using conditions C4 developed much higher stresses, and these values were more or less maintained unchanged on ageing at 0%RH with EP/H1, EP/H4 and EP/H5 (Fig. 16 and reference 7). With EP/H1 the stress remained tensile even while ageing at 97%RH in the free-to-bend state (Fig. 16). With

restrained substrate ageing at 97%RH, the stresses reversed to become compressive (Fig. 16). With EP/H2 the free-to-bend sample aged at 97%RH also developed compressive stresses (Fig. 17) and a further difference was that the restrained substrate sample showed a drop in (tensile) stress when aged at 0%RH (Fig. 17). EP/H3 gave very high tensile stresses after post-curing (Fig. 18). Even though the stresses in the coating on the free-to-bend substrate fell quite rapidly when exposed to humid air, the coatings peeled away from the substrate after approximately 20 days, presumably due to a combination of tensile stress and weakening of the interface due to the penetration of diffused water [7]. With EP/H4 and EP/H5 the behaviour was much more regular [7]. Little change in residual stress occurred when the coatings were aged at 0%RH, whereas the tensile stress present originally fell significantly when aged in humid air. The only sample that produced compressive stress was EP/H4, when aged at 97%RH [7]. The summary shown in Fig. 19 again reveals EP/H5 to be the least sensitive to ageing at different levels of humidity.

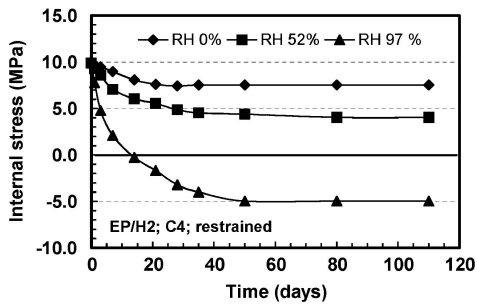
4. Discussion

4.1. Curing characteristics

The major purpose of the research described in this paper was to investigate the effect of different curing agents on the development of internal stresses during cure and on the subsequent changes in internal stresses caused by ageing at different level of humidity. In order

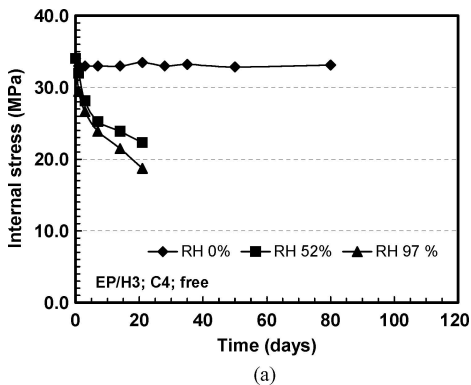


(a)

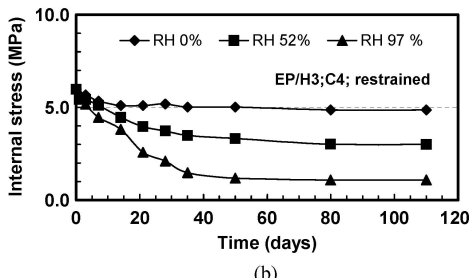


(b)

Figure 17 Internal stress development in EP/H2 post-cured using conditions C4 then stored at RH 0; 52; and 97% respectively. (a) Results obtained with free-to-bend substrate; (b) results obtained with restrained substrate.



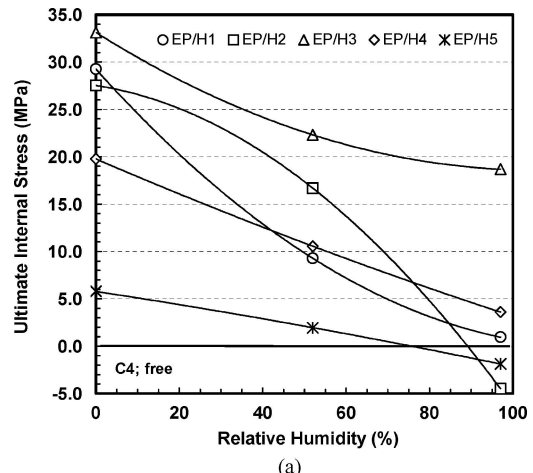
(a)



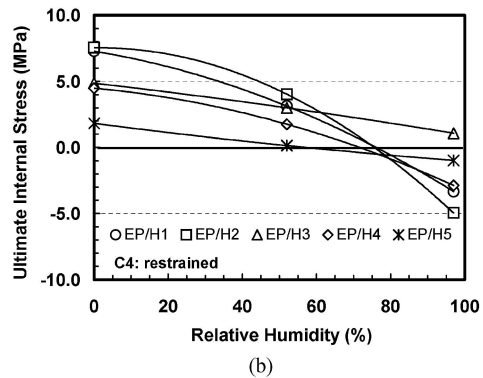
(b)

Figure 18 Internal stress development in EP/H3 post-cured using conditions C4 then stored at RH 0; 52; and 97% respectively. (a) Results obtained with free-to-bend substrate (note that samples exposed to 52%RH and 97%RH failed prematurely—see text); (b) results obtained with restrained substrate.

to interpret the internal stress measurements, it is necessary to consider first the state of cure of the materials and the nature of the changes that take place during curing.



(a)



(b)

Figure 19 Effect of relative humidity on the equilibrium (long ageing time) stress built up in coatings on (a) free-to-bend substrates and (b) restrained substrates stored at 0; 52; and 97%RH after post-cure conditions C4. Note that no values for EP/H3 are plotted in the free-to-bend graph because the samples delaminated before equilibrium was achieved when tests were conducted at 52%RH and 97%RH.

A suitable starting place is the curing cycle suggested by Shimbo *et al.* [11, 29, 30], illustrated in Fig. 20. This follows the density changes when an initially uncured epoxy compound starts at room temperature (T_r) at the state represented by A in Fig. 20. When the temperature is advanced to the curing temperature, T_c , the density falls (along AB) because of the process of thermal expansion. If the material is held at T_c for an extended period, the density increases with time (BC). On subsequent cooling, the density increases due to thermal contraction (C-D-E). The rate of increase with fall in temperature is lower when the temperature is below the glass transition temperature of the cured polymer, i.e. $T < T_g$ (DE) than when $T > T_g$ (CD). The end point, E, when the material has returned to room temperature, is above A due to the net shrinkage that has occurred.

The Shimbo model relates only to high temperature curing epoxy systems and does not fully describe the changes that occur during the curing and post-curing programme to which the materials were subjected to in the research described here. There are three features that are not present in Fig. 20. They are:

- (i) A degree of curing occurs at room temperature before the post-cure treatment;
- (ii) The room temperature curing will often be sufficient for network formation and the development

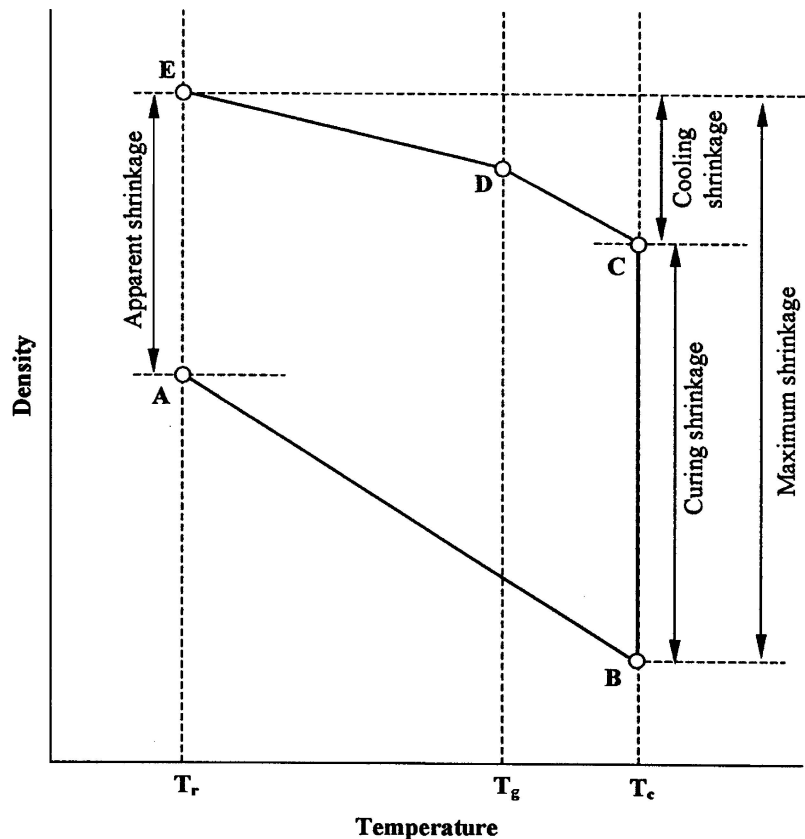


Figure 20 Curing cycle for an epoxy resin system, after Shimbo *et al.* [29, 30].

of a material with a glass transition temperature $T_g > T_r$;

(iii) After the post-cure, the T_g changes.

These features are shown in the scheme proposed in Fig. 21. The lettering used in Fig. 21 has been chosen to identify points common with the Shimbo model (Fig. 20). In Fig. 21, AE_1 represents the shrinkage that occurs during the initial room temperature curing. As temperature is advanced to T_c (E_1B) the material passes through T_g and the magnitude of the rate of change of density is higher in D_1B ($T > T_g$) than in E_1D_1 ($T < T_g$). The density increases during curing at $T = T_c$ (BC) and on cooling back to $T = T_r$ follow the same steps as those described above in the discussion of Shimbo's model (though note that in Fig. 21, the glass transition temperature during this phase of the temperature programme is written as T'_g to emphasize that it has changed since the beginning of the cure cycle). It is further noted that in many cases the glass transition temperature of the cured material was above T_c (see Fig. 5) and that point D_2 in Fig. 21 would not appear: CE_2 would then be a straight line, representing thermal shrinkage in the glassy state, $T < T'_g$, throughout this phase of the cycle.

The internal stresses that develop are related to the shrinkage components indicated in Fig. 21. It is noted, however, that Figs. 20 and 21 relate to volumetric changes and implicitly assume that the changes are permitted to occur at constant pressure. In the case investigated here the coating adheres strongly to a substrate that has a much smaller coefficient of thermal expansion and a much greater stiffness, and shrinkage

of the coating parallel to the interface with the substrate ($x - y$ plane) is severely restrained. This is the source of the internal stresses. The coating is unrestrained in the z -direction, however, and if molecular relaxation can take place, the material can change shape, so relieving the shrinkage stress. This process will be limited by the crosslinked network and will become progressively more difficult as cure proceeds. Relaxation will be very slow at $T < T_g$ even if the network has not developed fully.

4.2. Internal stresses in post-cured samples

The stresses present after post-curing contain contributions from the curing shrinkage and thermal shrinkage during the final part of the cycle, ($T_c - T_r$), modified by relaxation occurring at various phases of the cycle. If $T_r < T'_g < T_c$, the stress that develops during cooling ($C-D-E$ in Fig. 21) should be proportional to $\{\alpha_1(T_c - T'_g) + \alpha_2(T'_g - T_r)\}$ where α_1 is proportional to the thermal expansion coefficient when $T > T'_g$ and α_2 is proportional to the thermal expansion coefficient when $T < T'_g$. If $T'_g > T_c$ the stress due to cooling should be proportional to $\alpha_2(T_c - T_r)$. Samples for which $T'_g > T_c$ are easily identified by inspection of Fig. 5 (they lie above the broken line) and, if this contribution to the internal stress dominates, then removing data for all other samples from Fig. 6a and b should improve the straight line plots but no significant change is indicated when this action is taken. Therefore it is deduced that a significant contribution to the total internal stress accrues during curing. The difference in stresses measured in the free-to-bend and the restrained

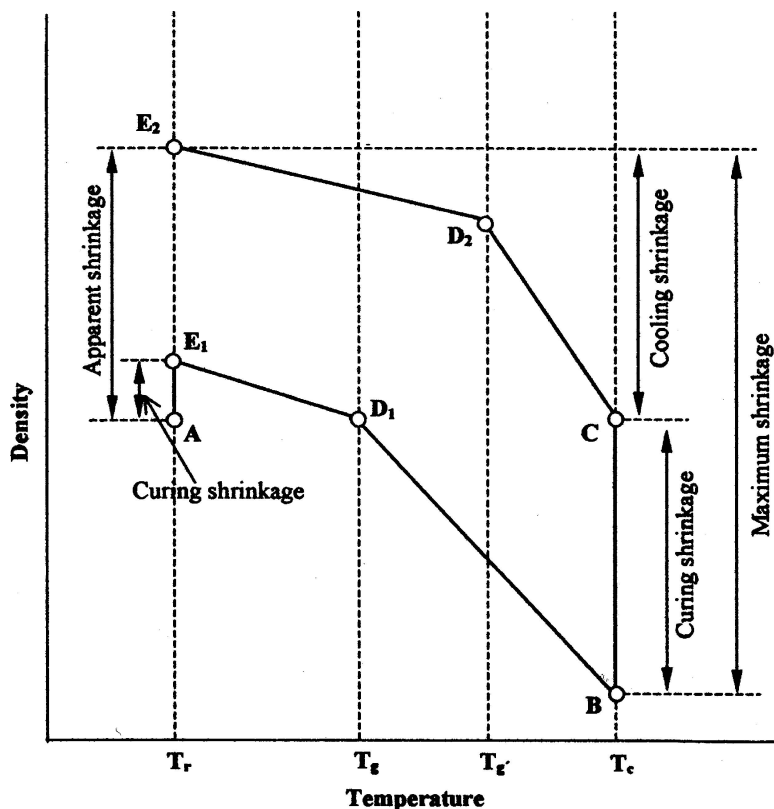


Figure 21 Modified curing cycle for epoxy resin allowed to solidify for a period at room temperature, T_r , during which it develops sufficient structural integrity to possess a glass transition temperature, T_g , then is post-cured at elevated temperature, during which time the glass transition temperature increases to T_g' .

substrate experiments has been attributed to changes that occur during curing [7] and this observation provides further evidence for the significant contribution to internal stress that is associated with curing.

From the results presented in Fig. 6 it is evident that the internal stresses developed during post-cure in EP/H5 (using polyamidoamine curing agent) were smaller than those observed in the other epoxy compositions. The internal stresses in compositions using curing agents DDM (H1), DETA (H2) and cycloaliphatic polyamine (H3) were much higher; composition EP/H4 (polyamidoamine curing agent based on IPD) developed stresses intermediate in magnitude (Fig. 6). H4 and H5 contain relatively long aliphatic chains. This probably accounts for the low glass transition temperatures T_g' developed in the corresponding epoxy compounds. Stress relaxation will occur more readily in the materials possessing low T_g' .

4.3. Internal stress development during ageing at different humidity levels

The absorption of water from humid air caused significant reductions in the tensile internal stresses and caused compressive stresses to develop in many cases (Figs. 8, 11, 15, 19). This is attributed to swelling caused by the penetrant. That this cannot be the only effect is indicated by a consideration of the results obtained with EP/H5. Ageing of the samples post-cured at room temperature caused only modest changes in the stress in EP/H5 and this material was the least affected by differences in humidity (Figs. 7, 8, 10, 11, 14, 15, 19: more

data are given in reference 7). However, when samples were immersed in water, the greatest uptake of water was observed with EP/H4, followed closely by EP/H5 [7, 31]. Water absorption in humid air may not follow exactly the pattern observed with total immersion, but it is unlikely that there will be a significant change of ranking in humid air and a different explanation for the stress observations should be sought. It is likely that the effect of water absorption is related instead to free volume and relaxation effects. The long aliphatic chains in H4 and H5 are responsible for the high free volume and low glass transition temperature and the presence of water will plasticize the material still further. The conditions therefore favour stress relaxation. It is likely that absorbed water will disrupt hydrogen bonding in EP/H5, reducing its capacity to develop stresses of large magnitude (either tensile or compressive).

Regarding the anomalous result obtained when ageing EP/H5 post-cured under conditions C3, (Section 3.4.3) it is not at all obvious why tensile stresses should develop when ageing following such a high temperature post-cure. It would be expected that this treatment would leave the material in such a state that there would be little opportunity for continued curing and any further shrinkage. One hypothesis is that water absorption facilitated molecular relaxation (possibly accompanied by further crosslinking, if there had remained unreacted groups that were trapped in the glassy phase), leading to volumetric shrinkage, as in physical ageing [28]. Another possibility is that water formed hydrogen bonding linkages between molecules so contributing to the shrinkage of the network. However, in all of the

other materials, exposure to water caused reduction in tensile stress; the stress often reversed, becoming compressive. It is therefore evident that, in all other experiments, the uptake of water caused swelling to dominate, even if a counter effect was also present.

4.4. Effect of substrate constraint

Further evidence for the influence of the substrate constraint on curing is given by the ultimate stress data in Figs. 8, 11, 14 and 19. The largest post-cure stresses and the largest changes in stresses on ageing were obtained with the highest post-cure temperature (150°C: C4; Fig. 19). The sequence of restrained substrate measurements shows more order than that for the free-to-bend experiments. The scatter bands containing the results for restrained substrate tests with C3 and C4 (Figs. 15b and 19b) almost superimpose; this probably reflects the observation that the samples are almost fully cured after both of these treatments [7]. Smaller stresses and smaller changes on ageing were recorded in restrained substrate samples cured according to treatments C1 and C2 (Figs. 8b and 11b). This is probably because of the greater relaxation allowed in samples following these post-cure treatments (see the T_g data in Fig. 5). With the free-to-bend samples the general trend is for the ultimate stress observed after an extended period of ageing to move to higher values as the post-cure temperature increases (Figs. 8a, 11a, 14a and 19a). This is presumably because the tensile stress at the end of the post-cure scaled with post-cure temperature. This does not explain why there is a difference in the relative changes observed for free-to-bend and restrained substrate testing for the different post-cure treatments. In the absence of further information, we can only speculate that the uptake of water depends on the stress in the coating (which is different for free-to-bend and restrained substrate testing) as well as the hardener used, and that a complex combination of these two effects must be responsible for the observations. This provides further reason to question the validity of free-to-bend internal stress measurements for the assessment of internal stresses in service situations that replicate more closely the restrained substrate test, which is normally the case.

5. Conclusions

- The internal stresses that develop when an epoxy compound is cured depend strongly on the nature of the curing agent;
- The stresses that develop in compounds based on different curing agents can be related to the molecular structure of the curing agent but, as yet, no quantitative method to predict the stress magnitudes from the molecular structure exists;
- The internal stresses depend on curing temperature but there is also a direct contribution from curing shrinkage and modification due to stress relaxation, and the various effects are difficult to separate and quantify;
- Ageing in humid air produces significant changes in internal stresses in most of the compounds tested

and can generally be explained qualitatively by swelling caused by water absorption;

- Some exceptions to the water swelling model are attributed tentatively to hydrogen bonding with the reacted curing agent molecules;
- There is no simple correlation between the stress magnitudes measured using the free-to-bend and restrained substrate tests;
- The restrained substrate method probably relates more closely to service conditions than the free-to-bend method, but the latter was found to produce failures (delamination) with coatings that did not fail on a restrained substrate when all other conditions were the same.

References

1. J. R. WHITE, *Polym. Test.* **4** (1984) 165 [Also appeared as Chapter 8 in "Measurement Techniques for Polymeric Solids," edited by R. P. Brown and B. E. Read (Elsevier, Barking, 1984)].
2. D. KOTNAROWSKA, *Prog. Org. Coat.* **37** (1999) 149.
3. S. G. CROLL, *J. Coatings Technol.* **51**(648) (1979) 64.
4. K. SATO, *Prog. Org. Coat.* **8** (1980) 143.
5. M. OOSTERBROEK, R. J. LAMMERS, L. G. T. VAN DER VEN and D. Y. PERERA, *J. Coat. Technol.* **63**(797) (1991) 55.
6. C. H. HARE, *J. Protect. Coat. Linings* **13** (1996) (Article in several parts) pp. 8, 10, 65, 99.
7. A. F. ABDELKADER, PhD thesis, University of Newcastle upon Tyne, 2003.
8. M. SHIMBO, M. OCHI and K. ARAI, *J. Coat. Technol.* **57**(728) (1985) 93.
9. GU YAN and J. R. WHITE, *Polym. Eng. Sci.* **39** (1999) 1866.
10. S. G. CROLL, *J. Coat. Technol.* **51**(659) (1979) 49.
11. M. SHIMBO, M. OCHI and K. ARAI, *ibid.* **56**(713) (1984) 45.
12. T. YOSHIDA, *Prog. Org. Coat.* **1** (1972) 73.
13. D. J. NEWMAN and C. J. NUNN, *ibid.* **3** (1975) 221.
14. T. KRZYZANOWSKA, *ibid.* **3** (1975) 349.
15. S. G. CROLL, *J. Coat. Technol.* **50**(638) (1978) 33.
16. *Idem.*, *ibid.* **51**(648) (1979) 64.
17. *Idem.*, *J. Appl. Polym. Sci.* **23** (1979) 847.
18. D. Y. PERERA and D. VAN DEN EYNDE, *J. Coat. Technol.* **55**(699) (1983) 37.
19. A. F. ABDELKADER and J. R. WHITE, *Prog. Org. Coat.* **44** (2002) 122.
20. D. Y. PERERA and D. VAN DEN EYNDE, *J. Coat. Technol.* **59**(748) (1987) 55.
21. K. SATO and Y. INOUE, *Shikizai Kyokaishi* **32** (1959) 394.
22. J. L. PROSSER, *Modern Paint Coat.* July (1977) 47.
23. O. NEGELE and W. FUNKE, *Prog. Org. Coat.* **28** (1996) 285.
24. S. G. CROLL, *J. Oil Colour Chemists' Assoc.* **63** (1980) 271.
25. D. Y. PERERA, in "Paint and Coatings Testing," edited by J. V. Koleske, ASTM 14th ed. Gardner-Sward Handbook, ASTM Manual Series, MNL 17 (1995) p. 585.
26. ASTM D3418-75, "Annual Book of ASTM Standards, 06.01," (American Society for Testing and Materials, 1993) p. 840.
27. A. F. ABDELKADER and J. R. WHITE, *J. Mater. Sci.* **37** (2002) 4769.
28. L. C. E. STRUIK, "Physical Aging in Amorphous Polymers and Other Materials" (Elsevier, Amsterdam, 1978).
29. M. SHIMBO, M. OCHI and Y. SHIGETA, *J. Appl. Polym. Sci.* **26** (1981) 2265.
30. M. SHIMBO, M. OCHI and T. INAMURA, *J. Mater. Sci.* **20** (1985) 2965.
31. A. F. ABDELKADER and J. R. WHITE, to be published.

Received 14 December
and accepted 16 December 2004